RESEARCH ARTICLE

A rapid micro-magnetic resonance imaging scanning for three-dimensional reconstruction of peripheral nerve fascicles

Zhi Yao[1,2,#], Li-Wei Yan[1,2,#], Tao Wang[1,2], Shuai Qiu[1,2], Tao Lin[1,2], Fu-Lin He[1,2], Ru-Heng Yuan[1,2], Xiao-Lin Liu[1,2,3], Jian Qi[1,2,3,*], Qing-Tang Zhu[1,2,3,*]
1 Department of Microsurgery and Orthopedic Trauma, First Affiliated Hospital of Sun Yat-sen University, Guangzhou, Guangdong Province, China
2 Center for Peripheral Nerve Tissue Engineering and Technology Research, Guangzhou, Guangdong Province, China
3 Guangdong Province Engineering Laboratory for Soft Tissue Biofabrication, Guangzhou, Guangdong Province, China

Funding: *This study was supported by grants from the National Key Research and Development Plan of China, No. 31670986 (to QTZ); the Science and Technology Project of Guangdong Province of China, No. 2014B020227001, 2017A050501017 (to QTZ); the Science and Technology Project of Guangzhou of China, No. 201807010082 (to QTZ), 201704030041 (to JQ).*

Graphical Abstract

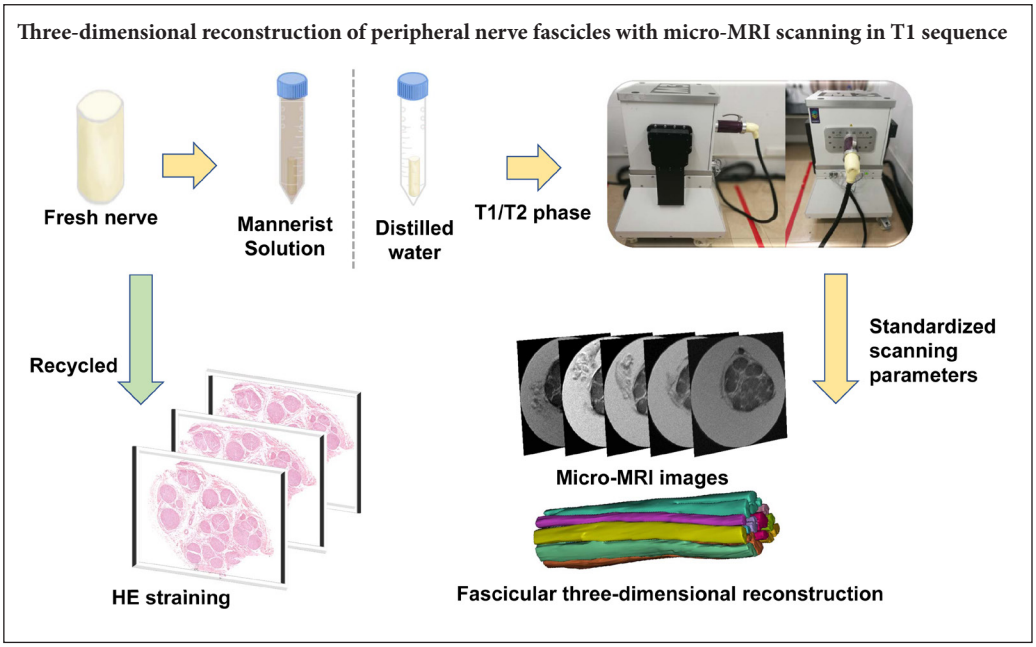

Correspondence to:
Qing-Tang Zhu, MD, PhD or Jian Qi, MD, PhD, zhuqingt@mail.sysu.edu.cn or speedsnow@126.com.

#These authors contributed equally to this study.

orcid:
0000-0001-6256-1602 (Qing-Tang Zhu)
0000-0003-4993-1335 (Jian Qi)

doi: *10.4103/1673-5374.238718*

Accepted: *2018-06-22*

Abstract

The most common methods for three-dimensional reconstruction of peripheral nerve fascicles include histological and radiology techniques. Histological techniques have many drawbacks including an enormous manual workload and poor image registration. Micro-magnetic resonance imaging (Micro-MRI), an emerging radiology technique, has been used to report results in the brain, liver and tumor tissues. However, micro-MRI usage for obtaining intraneural structures has not been reported. The aim of this study was to present a new imaging method for three-dimensional reconstruction of peripheral nerve fascicles by ^{1}T micro-MRI. Freshly harvested sciatic nerve samples from an amputated limb were divided into four groups. Two different scanning conditions (Mannerist Solution/GD-DTPA contrast agent, distilled water) were selected, and both T1 and T2 phases programmed for each scanning condition. Three clinical surgeons evaluated the quality of the images *via* a standardized scale. Moreover, to analyze deformation of the two-dimensional image, the nerve diameter and total area of the micro-MRI images were compared after hematoxylin-eosin staining. The results show that rapid micro-MRI imaging method can be used for three-dimensional reconstruction of the fascicle structure. Nerve sample immersed in contrast agent (Mannerist Solution/GD-DTPA) and scanned in the T1 phase was the best. Moreover, the nerve sample was scanned freshly and can be recycled for other procedures. MRI images show better stability and smaller deformation compared with histological images. In conclusion, micro-MRI provides a feasible and rapid method for three-dimensional reconstruction of peripheral nerve fascicles, which can clearly show the internal structure of the peripheral nerve.

Key Words: *nerve regeneration; peripheral nerve; fascicular three-dimensional reconstruction; fascicular topography; micro-magnetic resonance imaging; rapid acquired images; contrast agent; Mannerist Solution; histological techniques; deformation analysis; peripheral nerve injury; neural regeneration*

Introduction

Fascicular topography of peripheral nerves is complicated and their aggregation and distribution are still not completely known. However, increased understanding of peripheral nerve fascicular topography has important clinical and scientific significance. Therefore, novel research and technologies are particularly important. From a clinical perspective, knowledge of fascicular topography may benefit microsurgery (Terzis and Kostopoulos, 2007), oral and maxillofacial surgery (Terzis and Konofaos, 2008), and other surgical specialties including those for repair and reconstruction of peripheral nerve injury and nerve transposition repair to improve curative effects (Siqueira et al., 2010). In the field of bio-fabrication, and with the development of three-dimensional (3D) printing technology (Johnson et al., 2015), fascicular topography can provide information based on a mathematical model for design of a nerve scaffold. Thus, a 3D printed personalized nerve graft may be possible (Murphy and Atala, 2014).

The mainstream method for the study of peripheral nerve fascicular topography is histochemically stained serial sections (Delgado-Martínez et al., 2016). Yet during recent decades, the ability of computer-generated 3D medical image reconstruction has grown (Watchmaker et al., 1991). Studies have shown peripheral nerve anatomical 3D reconstruction using data from histological techniques. However, this method still requires substantial manual workload for image registration and contour acquisition, which not only increases work intensity but also reduces the accuracy of reconstructed fascicles (Pommert et al., 2006).

New medical radiology techniques, including microscopic-computed tomography (micro-CT) and microscopic-magnetic resonance imaging (micro-MRI), are expected to achieve technological breakthroughs for the study of fascicular topography (Gignac and Kley, 2014; Gignac et al., 2016). Researchers have previously reported iodine and freeze-drying enhanced high-resolution micro-CT imaging for reconstruction of 3D intraneural topography of human peripheral nerve fascicles (Zhu et al., 2016; Yan et al., 2017a, b, c). Nevertheless, deformation of nerve samples after iodine pretreatment and freeze-drying is inevitable for micro-CT scanning, and results in changes of physicochemical properties. Consequently, nerve samples cannot be recycled and used for other experiments. Micro-MRI is an emerging radiology technique that has been applied in the brain (Baltes et al., 2009), liver (Pandit et al., 2013), tumor tissue (Olson et al., 2012), and other soft tissue. Micro-MRI is a quantitative and qualitative assessment for local soft tissue edema and adhesions (Paredes et al., 2014), and can be used in combination with a contrast agent for microvascular imaging (Benoit et al., 2009) and pyramidal pathway imaging (Deans et al., 2015). In the field of neuroscience, micro-MRI can be used for evaluating repair of peripheral nerve injury in animal models *in vivo* (Liao et al., 2012), and provide a quantitative measurement that reflects nerve regeneration *via* local peripheral nerve T1 and T2 values (Shen et al., 2010). However, use of micro-MRI for obtaining intraneural structures has not been reported, and its potential remains to be investigated. The aim of this study was to determine the feasibility of micro-MRI for obtaining two dimensional (2D) continuous scanning images of peripheral nerve. By comparing the quality of scanning images in two different scanning conditions (Mannerist Solution/gadolinium-diethylenetriamine pentaacetic acid [GD-DTPA] contrast agent and distilled water) as well as 3D reconstruction of peripheral nerve fascicles, our study provides a new method for investigating the internal structure of peripheral nerve.

Materials and Methods

Human peripheral nerve samples

Human nerves were excised from the lower limb of three amputation patients at the First Affiliated Hospital of Sun Yat-sen University of China. All human experiments followed procedures approved by the Institutional Review Boards of the Contributing Institutions of the First Affiliated Hospital of Sun Yat-sen University in accordance with the *Declaration of Helsinki*. All donors provided informed consent for donation of their tissue for teaching and research purposes.

Selection of the lower extremity for harvesting nerve samples required no tumor infiltration, no serious soft tissue defects or contamination, no thrombosis in the main arteries of the lower extremities, and no obvious ischemic signs in the lower extremities before amputation.

Nutritional status of the patients was good or moderate (no significant cachexia in tumor patients). Sciatic nerves were harvested from three amputated limbs approximately 2 hours after the main artery was cut. Each sciatic nerve was cut into four short segments (2.5 cm). Sciatic nerves were carefully and appropriately pruned under a microscope, with the surrounding fat tissue removed.

Micro-MRI peripheral nerve scanning conditions and standardized scanning parameters

According to the imaging principle of MRI, two different scanning conditions were selected: one using contrast agent and the other using distilled water. This study used the contrast agent, GD-DTPA (Magnevist; Bayer Healthcare, Berlin, Germany) (molecular weight: 938 kDa, molecular formula: $C_{14}H_{20}GdN_3O_{10}{\cdot}2C_7H_{17}NO_5$), which is the most commonly used agent for enhanced-MRI. GD DTPA (0.1 mL) was dissolved in 50 mL iodide to obtain a contrast medium solution of 0.2% concentration. Both the T1 and T2 phases were programmed for the two scanning conditions.

To determine the optimized scanning condition for nerve scanning, the samples (n = 12; three nerves were obtained, with each nerve cut into four segments) were divided into four groups. The nerve sample was placed in the bottom of the scanning tube, and the tube filled with contrast agent or distilled water. After removing any bubbles, the tube was sealed. In group A, the nerve sample was immersed in contrast agent (Mannerist Solution/GD-DTPA) and scanned in the T1 phase. In group B, the nerve sample was immersed in contrast agent (Mannerist Solution/GD-DTPA) and

Table 1 Standardized scanning parameters

	A			B			C			D		
Slice orientation	Axial	Coronal	Sagittal	Axial	Coronal	Sagittal	Axial	Coronal	Sagittal	Axial	Coronal	Sagittal
Number of slices	25	13	13	25	13	13	25	13	13	25	13	13
Slices thickness (mm)	1	1	1	1	1	1	1	1	1	1	1	1
Inter-slice gap (mm)	0.1	0.1	0.1	0.1	0.1	0.1	0.1	0.1	0.1	0.1	0.1	0.1
Hor.FOV (mm)	15	12	12	15	12	12	15	12	12	15	12	12
Vert.FOV (mm)	15	25	25	15	25	25	15	25	25	15	25	25
# Phase encodings	300	240	240	288	240	240	300	240	240	288	240	240
# Sample	300	500	500	300	500	500	300	500	500	300	500	500
Repetition time (ms)	607.025	539.570	539.570	8715.800	6872.32	6872.320	607.025	539.570	539.570	8715.800	6872.320	6872.320
Echo time (ms)	15.834	23.706	23.706	66.366	69.388	69.388	15.834	23.706	23.706	66.366	69.388	69.388
Inversion time (ms)	100	100	100	100	100	100	100	100	100	100	100	100
Pixel size (mm)	0.05	0.05	0.05	0.05	0.05	0.05	0.05	0.05	0.05	0.05	0.05	0.05
# Excitations	50	50	50	50	50	50	50	50	50	50	50	50
Scan time	02:45:55	01:59:37	01:59:37	03:13:40	02:10:19	02:10:19	02:45:55	01:59:37	01:59:37	03:13:40	02:10:19	02:10:19

Axial, coronal, and sagittal views of each nerve sample were scanned. Scanning window size was determined by scout view. Scanning accuracy was 50 μm. Group A: nerve sample in Mannerist Solution scanned in T1 phase; Group B: nerve sample in Mannerist Solution scanned in T2 phase; Group C: nerve sample in distilled water scanned in T1 phase; and Group D: nerve sample in distilled water scanned in T2 phase. Hor. FOV: Horizontal field of view; Vert. FOV: vertical field of view.

Table 2 Standardized scale for evaluation of micro-MRI images

	Observer 1				Observer 2				Observer 3			
Group	A	B	C	D	A	B	C	D	A	B	C	D
Fascicles recognition capability (1–5)	4	2	2	3	4	2	3	4	4	3	2	4
Image stability (1–5)	5	4	2	5	5	3	2	4	4	4	3	4
Background noises (1–5)	4	4	4	4	4	3	4	3	4	3	3	4
Total score	13	10	8	12	13	8	9	11	12	10	8	12

Micro-MRI images were evaluated by three clinical surgeons with more than 20 years of experience. Each consideration factor (including Fascicle recognition capability, Image stability, and Background noise) was scored from 1 to 5. Group A: nerve sample in Mannerist Solution scanned in T1 phase; Group B: nerve sample in Mannerist Solution scanned in T2 phase; Group C: nerve sample in distilled water scanned in T1 phase; and Group D: nerve sample in distilled water scanned in T2 phase. Micro-MRI: Microscopic-magnetic resonance imaging.

scanned in the T2 phase. In group C, the nerve sample was immersed in distilled water and scanned in the T1 phase. In group D, the nerve sample was immersed in distilled water and scanned in the T2 phase. After sample preparation, the tube was placed into the head coil of the micro-MRI (M3; Aspect Imaging, Jerusalem, Israel). The scanning parameters are listed in **Table 1**.

Deformation analysis using histological techniques

Deformation of micro-MRI 2D images was analyzed by hematoxylin-eosin staining. Nerve samples were immediately recycled after micro-MRI scanning. Thus, the same nerve sample was first scanned by micro-MRI and then cut into serial sections followed by hematoxylin-eosin staining. Nerves were fixed in 4% paraformaldehyde for 2 hours, followed by several washes in PBS for 24 hours. Fixed nerves were dehydrated using a graded series of ethanol, embedded in paraffin wax, transversely sectioned, and cut to a thickness of 3 mm using a cryostat (CM3050s; Leica, Wetzlar, Germany), and mounted on microscope slides. Sections were stained with hematoxylin and eosin to visualize the transverse nerve structure. The diameter and total area of the nerve were measured. The nerve diameter was the mean of the major and minor diameters. All measurements were performed using ImageJ software (NIH, Bethesda, MD, USA). The actual size was corrected according to the image scale, and the nerve area and diameter measured using an area selection tool and straight line tool.

Assessment of micro-MRI images and 3D reconstruction of peripheral nerve fascicles

To determine deformation of our scanning methods, after obtaining micro-MRI images, the sample was fixed and serial histological sections cut. Data were collected and image quality evaluated by three clinical surgeons from the Department of Microsurgery. The observers were blinded to the scanning conditions. A standardized scale (**Table 2**) was designed and used to evaluate 2D images. Fascicle recognition capability, image stability, and background noise were the main factors used to evaluate images. One group of continu-

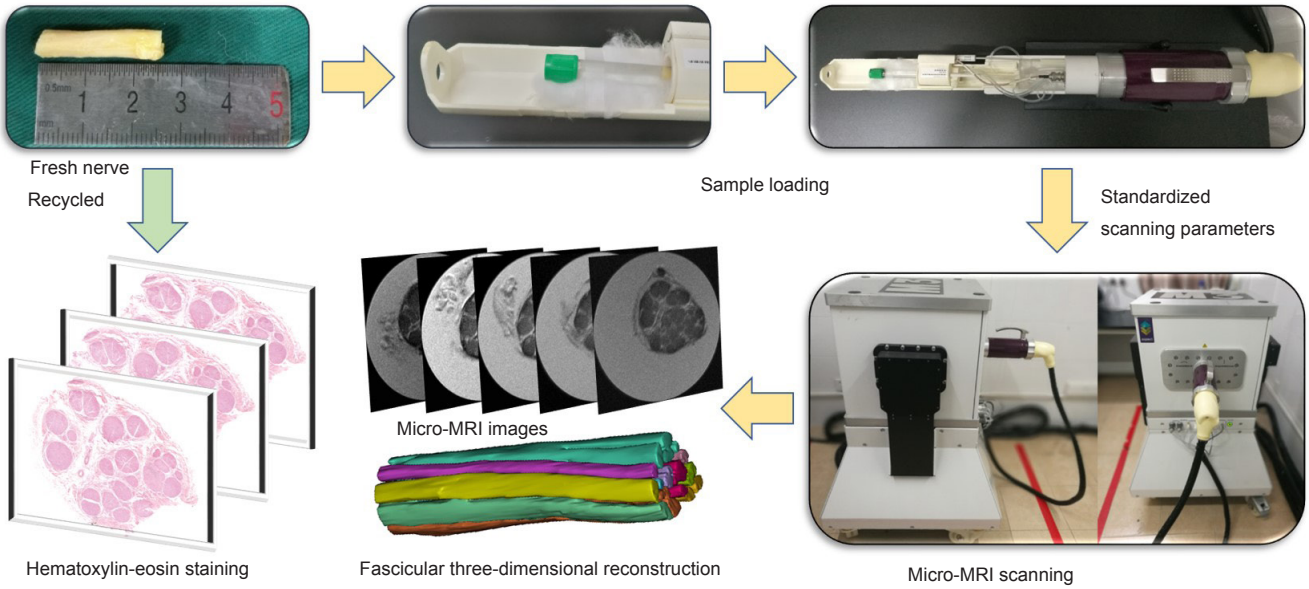

Figure 1 Schematic views of our rapid micro-MRI nerve scanning method for three-dimensional reconstruction of peripheral nerve fascicles.
Micro-MRI: Microscopic-magnetic resonance imaging.

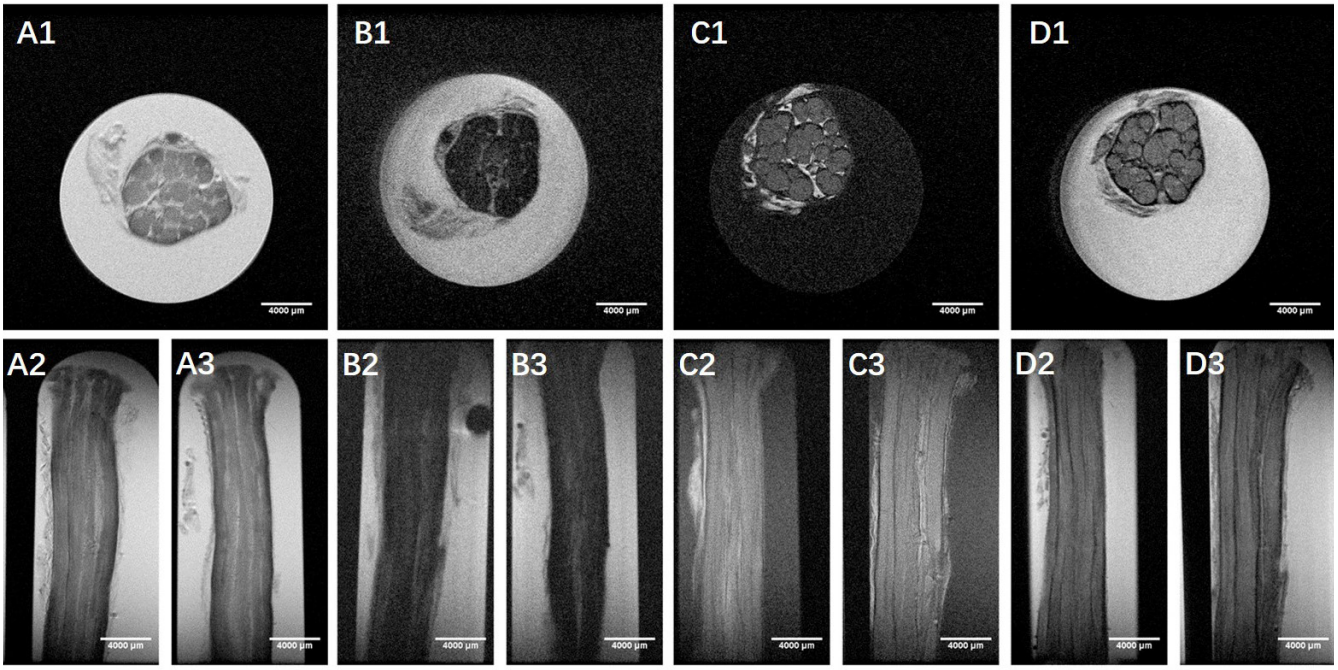

Figure 2 Micro-MRI scanning images.
Group A: The nerve sample was immersed in contrast agent (Mannerist Solution) and scanned in the T1 phase. Group B: The nerve sample was immersed in contrast agent (Mannerist Solution) and scanned in the T2 phase. Group C: The nerve sample was immersed in distilled water and scanned in the T1 phase. Group D: The nerve sample was immersed in distilled water and scanned in the T2 phase. A1, B1, C1, D1: Axial images; A2, B2, C2, D2: sagittal images; A3, B3, C3, D3: coronal images. Micro-MRI: Microscopic-magnetic resonance imaging.

ously scanned images was selected for 3D reconstruction of peripheral nerve fascicles. Data were collected and imported into software (Mimics Research 19.0; Materialise, Brussels, Belgium) for segmentation and 3D reconstruction of peripheral nerve fascicles. The threshold range (maximum threshold range that can segment fascicle area) was narrowed and a mask created. The mask was then split and irrelevant areas removed. Nerve fascicle boundaries were artificially optimized. Each fascicle was precisely segmented using logical operations and region growing.

Statistical analysis

Data are represented as the mean ± SD, and were analyzed using SPSS 24.0 software package for Windows (IBM, Ar-

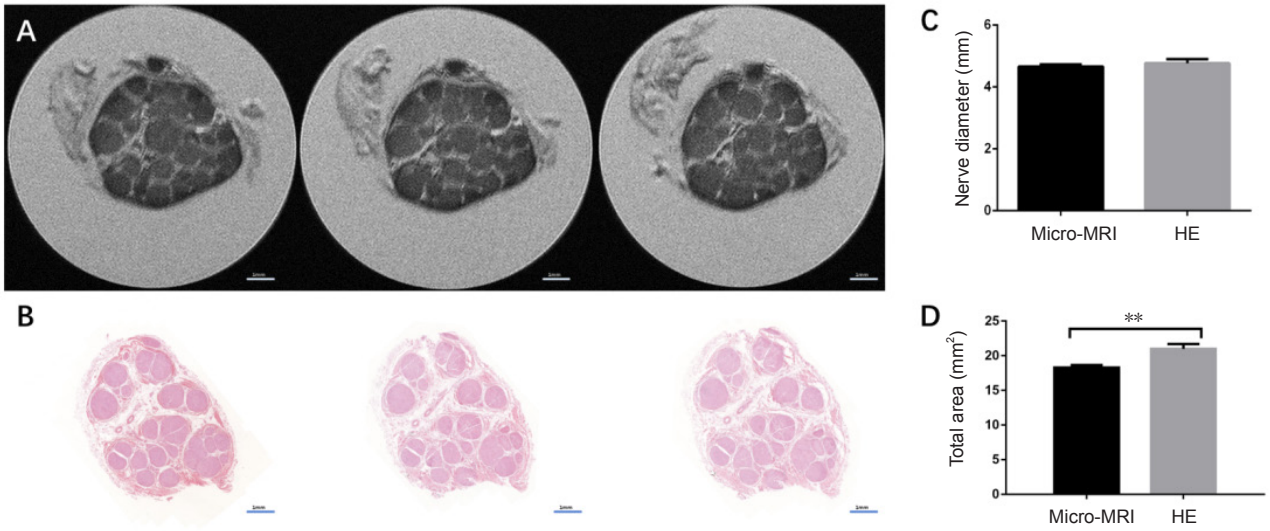

Figure 3 Deformation analyses of micro-MRI scanning images and HE staining histological section images.
The same nerve sample was first scanned by micro-MRI and then cut into serial sections, with HE staining used to compare images of both methods. (A) Micro-MRI scanning images. Scale bars: 1 mm. (B) Histological sections of HE stained images. Scale bars: 1 mm. (C) Comparison of nerve diameters in both image groups. (D) Comparison of total nerve area in both image groups. Student's *t*-test was used to examine the statistical significance of differences between sample means. Data are expressed as the mean ± SD. $^{**}P < 0.01$. Micro-MRI: Microscopic-magnetic resonance imaging; HE: hematoxylin-eosin.

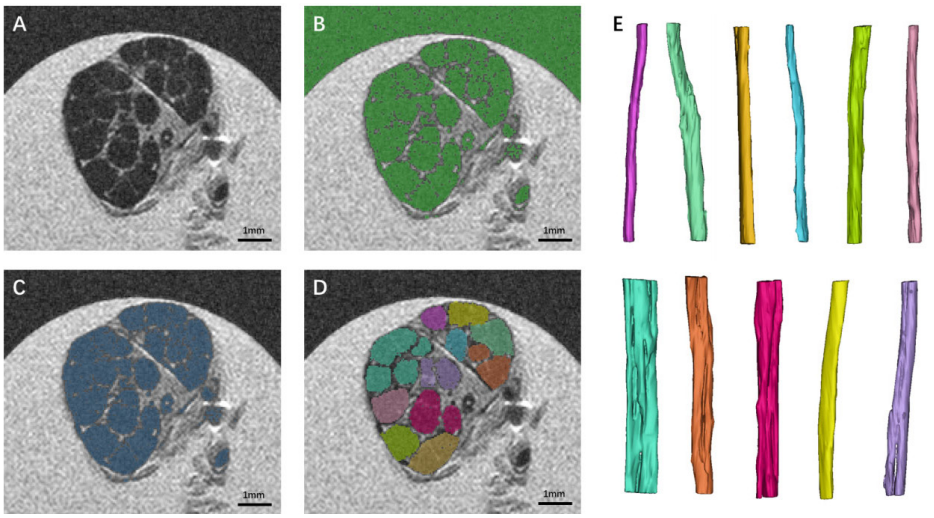

Figure 4 Segmentation of two-dimensional micro-MRI images.
(A) Original micro-MRI scanning images. (B) A narrowed threshold range and mask were created to identify segmentation fascicle area. (C) Split mask for removal of irrelevant areas. (D) Artificially optimized boundaries of nerve fascicles. Scale bars: 1 mm. (E) Each fascicle was precisely segmented using logical operations and region growing. Different colors were randomly chosen to illustrate the segmentation process of micro-MRI images, with different fascicles shown in various colors to ensure that the quality of micro-MRI images meet the requirements for fascicular segmentation. Micro-MRI: Microscopic-magnetic resonance imaging.

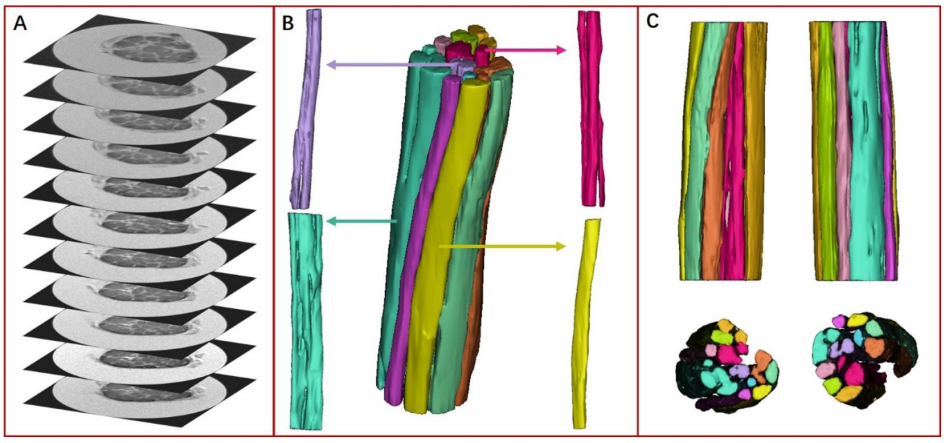

Figure 5 Three-dimensional reconstruction of peripheral nerve fascicles based on micro-MRI scanning images.
(A) Original micro-MRI scanning image (T1 phase images of nerve sample immersed in contrast agent). (B) Overall view of the nerve fascicle reconstruction model. Each individual fascicle can be observed and independently analyzed, clearly showing morphology, aggregation, and distribution. Arrows show the four different types of fascicular topography. (C) The reconstructed fascicular model is presented from different angles (left, right, top, and bottom). Different fascicles in various colors (each color is the same as which in Figure 4) show whether the quality of micro-MRI images meets the requirements for three-dimensional reconstruction. Micro-MRI: Microscopic-magnetic resonance imaging.

monk, NY, USA). Student's *t*-test was used to determine the statistical significance of differences between sample means. Values of $P < 0.05$ and < 0.01 were considered statistically significant.

Results

Rapid micro-MRI peripheral nerve scanning images and quality evaluation

Freshly harvested human sciatic nerves from amputated limbs were cut into 2.5 cm segments. Nerve samples in all groups followed the protocol outlined in **Figure 1**, including micro-MRI scanning following by serial sectioning and hematoxylin-eosin staining. Samples in all four groups underwent continuous scanning (**Figure 2**) with a scanning accuracy of 50 μm. For groups A and B, nerve samples were immersed in Mannerist Solution contrast agent and scanned in T1 and T2 phases. Fascicular area showed a low signal, while the scanning background had a high signal. For groups C and D, nerve samples were immersed in distilled water and scanned in T1 and T2 phases. Fascicular area exhibited a higher signal, while the scanning background showed a lower signal. Nerve fascicles could be manually identified in all groups.

Deformation comparison between micro-MRI and hematoxylin-eosin staining

After micro-MRI scanning, the nerve sample was cut into serial sections and stained with hematoxylin and eosin to compare images using both methods. Images displayed great similarity in morphology. Nerve diameter and total nerve area were measured to examine deformation (**Figure 3**). Diameter measured from micro-MRI images was 4.66 ± 0.07 mm, which was not significantly different from that measured from hematoxylin-eosin stained images (4.76 ± 0.13 mm). Total area of micro-MRI images was 18.28 ± 0.38 mm^2, which was significantly reduced compared with hematoxylin-eosin stained image areas, which measured 20.99 ± 0.70 mm ($P < 0.01$). These data demonstrate that MRI imaging shows good stability and results in less sample deformation.

Segmentation and 3D reconstruction of peripheral nerve fascicles

Micro-MRI images were evaluated by three clinical surgeons with more than 20 years of experience. The surgeons scored each consideration factor from 1 to 5. Group A was considered the best among all groups with a mean score of 12.6, while mean scores in other groups were: 9.3 (B), 8.3 (C), and 11.6 (D). Group A (scanning condition: contrast agent, T1 phase) was selected for 3D reconstruction of peripheral nerve fascicles (**Figures 3–5**). Each fascicle was observed and analyzed independently. Color-coded 3D models clearly identified morphology, aggregation, and distribution. Application of a semi-automatic segmentation method *via* Mimics software met the requirements for 3D reconstruction of nerve fascicles.

Discussion

Understanding of fascicular topography of peripheral nerves can ensure correct matching of nerve fascicles in nerve repair, which will maximize growth efficiency of axons and matching of fiber type during nerve regeneration. During nerve transposition repair, surgeons must combine topological information of nerve fascicles to minimize injury of donor nerve function and improve recovery of nerve function in recipient areas (Terzis and Kostopoulos, 2007). In the clinic, surgical repair after brachial plexus injury is an example of this application. Siqueira et al. (2010) reported a microanatomical study of the intraplexal topography of the suprascapular nerve, which may benefit suprascapular nerve reconstruction using a sural nerve graft. Their results showed that coaptation should be performed in the rostroventral quadrant of the C5 cross-sectional area (between 9 and 12 o'clock from the nerve surgeon's perspective in a right-sided brachial plexus exploration), which may minimize axonal misrouting and improve outcome (Siqueira et al., 2010). In addition, study of peripheral nerve fascicular topography will reduce iatrogenic nerve injury during surgery. In oral and maxillofacial surgery, there are reports on topological structure of the facial nerve. For nerve transposition and repair in patients with facial paralysis, the selected motor nerve must provide strong muscle contraction to allow patients to control facial movement. Therefore, it is crucially important to locate motional components of transposition nerve tracts. Accordingly, topological structure of nerve bundles can help optimize function matching (Hur et al., 2013).

An urgent problem in the field of peripheral nerve surgery is the lack of biomimetic nerve grafts to repair long segments of peripheral nerve defects. In different clinical conditions, the location, range, and nature of nerve injury can vary greatly from individual to individual (Scheib and Hoke, 2013; Jones et al., 2016). Thus, no existing nerve grafts (autologous nerve, multi-channel catheter, or acellular nerve grafts) can achieve satisfactory matching (Wegst et al., 2015). As tissue engineering develops, design and clinical application of individualized precise medical nerve grafts will be the future trend for treatment of peripheral nerve injury (Gu et al., 2014). Personalized nerve grafts based on 3D printing can precisely match the nerve structure around the defect, and have shown good application, prospect, and value (Hu et al., 2016). Tissue-engineered nerve grafts show potential as alternatives to existing nerve grafts (Feng et al., 2017). Our previous studies have shown significant differences of inner fascicular topography among different types of peripheral nerves, and indeed different levels in the same nerve (Zhong et al., 2015). Moreover, in a sciatic nerve defect animal model, we found that precisely matching fascicles can enhance the repair capacity of autologous nerve grafts for peripheral nerve injury (Yan et al., 2017a, b c). The results of this study provide a theoretical basis for future tissue-engineered nerve graft designs, including biomimetic fascicle pathways for repairing long nerve defects. Lack of extensive

data on inner fascicular topography of peripheral nerves and nerve manufacturing deficiencies are two bottlenecks that must be solved before creating biomimetic peripheral nerve grafts.

The study of fascicular topography is far from satisfactory. Emerging imaging technologies, including micro-CT and micro-MRI, provide new research methods but have limitations. Micro-CT can provide high-resolution imaging of peripheral nerve internal submicroscopic structures, and its high fidelity and continuous imaging provide a reliable support for establishment of a digital information bank for peripheral nerve anatomical microstructures. Micro-CT peripheral nerve scanning still faces technical problems, including enhancement and optimization of images, deformation after pretreatment of nerve samples, 2D image optimization for 3D reconstruction, and a massive demand for hardware and software. Although this method provides a better means of obtaining peripheral nerve topology, future research efforts that include integrating various methods, minimizing nerve sample deformation, and permitting sample reutilization, will provide more accurate fascicular topology. Nonetheless, this is the first study to report intraneural images acquired *via* micro-MRI technology. Neuroimaging has always been very challenging for clinical radiology. Although MRI has shown advantages in soft tissue imaging, intraneural scanning has yet to be accomplished because of its low contrast ratio and resolution. This study achieved rapid micro-MRI nerve scanning using standardized scanning parameters and optimized scanning conditions. Further, the images can be used for 3D reconstruction of peripheral nerve fascicles. Nerve samples were preserved and freshly scanned. Due to the rapid scanning time, sample deformation caused by swelling was minimized. Using this protocol, nerve samples can be used for other procedures.

The MRI device used in this study can only be used with semi-automatic manual segmentation. Micro-MRI has been used as a quantitative and qualitative assessment in many studies, and many MRI devices for scientific research have reached 7T (Olson et al., 2012), which presents high sensitivity and has many indications (Obusez et al., 2016; Cong et al., 2017). We expect that use of an upgraded MRI device in the future will provide fascicular scanning images with improved resolution. Other factors such as concentration of the contrast agent, size of the sample and scanning coil will provide even more significance. Another drawback of our study is that we cannot obtain long segment (> 5 cm) reconstruction of fascicular structure, because of the limitation of scanning bin size. Indeed, the current level of research can only be used to scan short nerve segments using radiology methods. It will be challenging to solve the following problems: (1) image mosaicism; (2) specimen deformation; and (3) fascicle matching and positioning between segments. To analyze the fascicle pattern and trace to target organs, long segment reconstruction of fascicular structure and massive data collection are essential. Hence, numerous technical difficulties still need to be solved in actual practice.

In summary, the rapid micro-MRI nerve scanning method described in this study facilitates acquisition of the 3D topography of peripheral nerve fascicles, which may improve understanding of neurobiological principles and guide accurate nerve transposition repair. The 3D fascicular model can be used as a bio-fabrication model, which presents a good solution for long nerve gap repairs. This method has more potential applications when combined with higher power micro-MRI equipment. Future studies analyzing peripheral nerve microstructure still require the combination of various technologies.

Author contributions: *ZY and QTZ designed and conceived the study and wrote the manuscript. ZY, LWY conducted micro-MRI scanning and obtained 2D images. SQ, JQ, and XLL analyzed the data and reconstructed the fascicles of peripheral nerve. FLH and RHY analyzed the deformation of the nerve images. TW and TL modified the manuscript. All authors discussed the conceptual and practical implications of the methods, and approved the final version of the paper.*
Conflicts of interest: *The authors have no conflicts of interest to declare.*
Financial support: *This study was supported by grants from the National Key Research and Development Plan of China, No. 31670986 (to QTZ); the Science and Technology Project of Guangdong Province of China, No. 2014B020227001, 2017A050501017 (to QTZ); the Science and Technology Project of Guangzhou of China, No. 201807010082 (to QTZ); the Science and Technology Project of Guangzhou of China, No. 201704030041 (to JQ). The funding bodies played no role in the study design, in the collection, analysis and interpretation of data, in the writing of the paper, and in the decision to submit the paper for publication.*
Institutional review board statement: *This study will be performed in strict accordance with the Declaration of Helsinki and relevant applicable ethical requirements. The study protocol was approved by the Ethics Committee of the First Affiliated Hospital of Sun Yat-sen University of China.*
Declaration of patient consent: *The authors certify that they have obtained patient consent forms. In the form, patients have given their consent for their images and other clinical information to be reported in the journal. The patients will understand that their names and initials will not be published and due efforts will be made to conceal their identity, but anonymity cannot be guaranteed.*
Reporting statement: *This study followed the Recommendations for the Conduct, Reporting, Editing and Publication of Scholarly Work in Medical Journals developed by the International Committee of Medical Journal Editors.*
Biostatistics statement: *The statistical methods of this study were reviewed by the biostatistician of the First Affiliated Hospital of Sun Yat-sen University of China.*
Copyright license agreement: *The Copyright License Agreement has been signed by all authors before publication.*
Data sharing statement: *Individual participant data that underlie the results reported in this article, after de-identification (text, tables, figures, and appendices) will be available. Study protocol, informed consent, and clinical study report will be available in September 2020. Anonymized trial data will be available indefinitely at http://www.jsxyfy.com.*
Plagiarism check: *Checked twice by iThenticate.*
Peer review: *Externally peer reviewed.*

Open peer reviewer: *Carolyn Tallon, Johns Hopkins University, USA.*
Additional file: *Open peer review report 1.*

References

Baltes C, Radzwill N, Bosshard S, Marek D, Rudin M (2009) Micro MRI of the mouse brain using a novel 400 MHz cryogenic quadrature RF probe. Nmr Biomed 22:834-842.

Benoit A, Guerard S, Gillet B, Guillot G, Hild F, Mitton D, Perie JN, Roux S (2009) 3D analysis from micro-MRI during in situ compression on cancellous bone. J Biomech 42:2381-2386.

Cong F, Zhuo Y, Yu S, Zhang X, Miao X, An J, Wang S, Cao Y, Zhang Y, Song HK, Wang DJ, Yan L (2017) Noncontrast-enhanced time-resolved 4D dynamic intracranial MR angiography at 7T: a feasibility study. J Magn Reson Imaging doi: 10.1002/jmri.25923.

Deans AE, Wadghiri YZ, Aristizabal O, Turnbull DH (2015) 3D mapping of neuronal migration in the embryonic mouse brain with magnetic resonance microimaging. Neuroimage 114:303-310.

Delgado-Martínez I, Badia J, Pascual-Font A, Rodríguez-Baeza A, Navarro X (2016) Fascicular topography of the human median nerve for neuroprosthetic surgery. Front Neurosci 10:286.

Feng C, Zhang W, Deng C, Li G, Chang J, Zhang Z, Jiang X, Wu C (2017) 3D printing of lotus root-like biomimetic materials for cell delivery and tissue regeneration. Adv Sci 4:1700401.

Gignac PM, Kley NJ (2014) Iodine-enhanced micro-CT imaging: methodological refinements for the study of the soft-tissue anatomy of post-embryonic vertebrates. J Exp Zool 322:166.

Gignac PM, Kley NJ, Clarke JA, Colbert MW, Morhardt AC, Cerio D, Cost IN, Cox PG, Daza JD, Early CM, Echols MS, Henkelman RM, Herdina AN, Holliday CM, Li Z, Mahlow K, Merchant S, Muller J, Orsbon CP, Paluh DJ, et al. (2016) Diffusible iodine-based contrast-enhanced computed tomography (diceCT): an emerging tool for rapid, high-resolution, 3-D imaging of metazoan soft tissues. J Anat 228:889-909.

Gu X, Ding F, Williams DF (2014) Neural tissue engineering options for peripheral nerve regeneration. Biomaterials 35:6143-56.

Hu Y, Wu Y, Gou Z, Tao J, Zhang J, Liu Q, Kang T, Jiang S, Huang S, He J, Chen S, Du Y, Gou M (2016) 3D-engineering of cellularized conduits for peripheral nerve regeneration. Sci Rep 6:32184.

Hur M, Kim H, Won S, Hu K, Song W, Koh K, Kim H (2013) Topography and spatial fascicular arrangement of the human inferior alveolar nerve. Clin Implant Dent R 15:88-95.

Johnson BN, Lancaster KZ, Zhen G, He J, Gupta MK, Kong YL, Engel EA, Krick KD, Ju A, Meng F, Enquist LW, Jia X, McAlpine MC (2015) 3D printed anatomical nerve regeneration pathways. Adv Funct Mater 25:6205-6217.

Jones S, Eisenberg HM, Jia X (2016) Advances and future applications of augmented peripheral nerve regeneration. Int J Mol Sci 17.

Liao CD, Zhang F, Guo RM, Zhong XM, Zhu J, Wen XH, Shen J (2012) Peripheral nerve repair: monitoring by using gadofluorine M-enhanced MR imaging with chitosan nerve conduits with cultured mesenchymal stem cells in rat model of neurotmesis. Radiology 262:161-171.

Murphy SV, Atala A (2014) 3D bioprinting of tissues and organs. Nat Biotechnol 32:773-785.

Obusez EC, Lowe M, Oh SH, Wang I, Jennifer B, Ruggieri P, Hill V, Lockwood D, Emch T, Moon D, Loy G, Lee J, Kiczek M, Manoj M, Statsevych V, Stultz T, Jones SE (2016) 7T MR of intracranial pathology: preliminary observations and comparisons to 3T and 1.5T. Neuroimage 168:459-476.

Olson JD, Walb MC, Moore JE, Attia A, Sawyer HL, McBride JE, Wheeler KT, Miller MS, Munley MT (2012) A gated-7T MRI technique for tracking lung tumor development and progression in mice after exposure to low doses of ionizing radiation. Radiat Res 178:321-327.

Pandit P, Johnston SM, Qi Y, Story J, Nelson R, Johnson GA (2013) The utility of micro-CT and MRI in the assessment of longitudinal growth of liver metastases in a preclinical model of colon carcinoma. Acad Radiol 20:430-439.

Paredes JL, Orabi AI, Ahmad T, Benbourenane I, Tobita K, Tadros S, Bae KT, Husain SZ (2014) A non-invasive method of quantifying pancreatic volume in mice using micro-MRI. PLoS One 9:e92263.

Pommert A, Hohne KH, Burmester E, Gehrmann S, Leuwer R, Petersik A, Pflesser B, Tiede U (2006) Computer-based anatomy a prerequisite for computer-assisted radiology and surgery. Acad Radiol 13: 104-112.

Scheib J, Hoke A (2013) Advances in peripheral nerve regeneration. Nat Rev Neurol 9:668-676.

Shen J, Zhou CP, Zhong XM, Guo RM, Griffith JF, Cheng LN, Duan XH, Liang BL (2010) MR neurography: T1 and T2 measurements in acute peripheral nerve traction injury in rabbits. Radiology 254:729-738.

Siqueira MG, Foroni LH, Martins RS, Chadi G, Malessy MJA (2010) Fascicular topography of the suprascapular nerve in the C5 root and upper trunk of the brachial plexus: a microanatomic study from a nerve surgeon's perspective. Neurosurgery 67:s402-406.

Terzis JK, Konofaos P (2008) Nerve transfers in facial palsy. Facial Plast Surg 24:177-193.

Terzis JK, Kostopoulos VK (2007) The surgical treatment of brachial plexus injuries in adults. Plast Reconstr Surg 119:73e-92e.

Watchmaker GP, Gumucio CA, Crandall RE, Vannier MA, Weeks PM (1991) Fascicular topography of the median nerve: a computer based study to identify branching patterns. J Hand Surg Am 16:53-59.

Wegst UG, Bai H, Saiz E, Tomsia AP, Ritchie RO (2015) Bioinspired structural materials. Nat Mater 14:23-36.

Yan L, Guo Y, Qi J, Zhu Q, Gu L, Zheng C, Lin T, Lu Y, Zeng Z, Yu S, Zhu S, Zhou X, Zhang X, Du Y, Yao Z, Lu Y, Liu X (2017a) Iodine and freeze-drying enhanced high-resolution MicroCT imaging for reconstructing 3D intraneural topography of human peripheral nerve fascicles. J Neurosci Meth 287:58-67.

Yan L, Qi J, Zhu S, Lin T, Zhou X, Liu X (2017b) 3D micro CT imaging of the human peripheral nerve fascicle. Int J Clin Exp Med 10:10315-10323.

Yan L, Yao Z, Lin T, Zhu Q, Qi J, Gu L, Fang J, Zhou X, Liu X (2017c) The role of precisely matching fascicles in the quick recovery of nerve function in long peripheral nerve defects. Neuroreport 28:1008-1015.

Zhong Y, Wang L, Dong J, Zhang Y, Luo P, Qi J, Liu X, Xian CJ (2015) Three-dimensional reconstruction of peripheral nerve internal fascicular groups. Sci Rep 5:17168.

Zhu S, Zhu Q, Liu X, Yang W, Jian Y, Zhou X, He B, Gu L, Yan L, Lin T, Xiang J, Qi J (2016) Three-dimensional reconstruction of the microstructure of human acellular nerve allograft. Sci Rep 6:30694.

(Copyedited by James R, Maxwell R, Wang J, Li CH, Qiu Y, Song LP, Zhao M)